

# Regional Climate Model Simulations of the 1998 Summer China Flood: Dependence on Initial and Lateral Boundary Conditions

Shuyan Liu<sup>\*1</sup>, Xin-Zhong Liang<sup>1,2</sup>, Wei Gao<sup>3,4</sup>, Yuxiang He<sup>1</sup>, Tiejun Ling<sup>5</sup>

<sup>1</sup>Earth System Science Interdisciplinary Center, University of Maryland, USA

<sup>2</sup>Department of Atmospheric and Oceanic Sciences, University of Maryland, USA

<sup>3</sup>USDA-UVB Monitoring and Research Program, Natural Resource Ecology Laboratory, Colorado State University, Fort Collins, USA

<sup>4</sup>Joint Laboratory for Environmental Remote Sensing and Data Assimilation, East China Normal University and Center for Earth Observation and Digital Earth, Chinese Academy of Sciences, Shanghai, China

<sup>5</sup>National Marine Environmental Forecasting Center, Beijing, China

**Abstract:** The dependence of the RegCM3 (Regional Climate Model version 3) downscaling skill on initial conditions (ICs) and lateral boundary conditions (LBCs) are investigated for the 1998 summer flood along the Yangtze River Basin in China. The effect of IC uncertainties is depicted by 15 realizations starting on each consecutive day from April 1 to 15 while all ending on September 1, 1998 with identical driving LBCs, analyses are based on June, July and August simulations. The result reveals certain IC effect on precipitation for daily evolution but little for summer mean geographical distribution. In contrast, the effect of LBCs uncertainties as represented by four different reanalyses are notably larger in both daily evolution and summer mean distribution. The ensemble average among either 15 IC realizations or 4 LBC runs does not show important skill improvement over the individuals. None of the RegCM3 simulations (including the ensemble means) captured the observed main rain band along the Yangtze River Basin. This general failure suggests the need for further model physics improvement.

**Keywords:** Ensemble, Initial condition, Lateral boundary condition, RegCM, regional climate model, Yangtze River Basin.

## 1. INTRODUCTION

Since Lorenz [1] first found that the atmosphere is a highly nonlinear system causing numerical solutions to be sensitive to small perturbations in initial conditions (ICs), and as computational capability is rapidly increasing, ensemble weather forecasts are becoming a common operational practice (Toth and Kalnay [2]; Mullen *et al.* [3]). A similar procedure has now also been taken in the general circulation model (GCM) community to construct ensemble climate predictions.

A Regional Climate Model (RCM) not only requires ICs at the initial step, but also time-dependent lateral boundary conditions (LBCs) which provide large-scale atmospheric circulation through buffer zones that drive the development of mesoscale systems inside the RCM domain. Both ICs and LBCs can be provided by GCM simulations. Since LBCs are required throughout the integration period, LBC-related errors can have long-term and damaging effects on RCM results (Warner *et al.* [6]). Effective LBC data assimilation techniques that accurately integrate LBCs across the buffer zones and a physically-based domain design critically determine the RCM performance (Liang *et al.* [4]). On the

other hand, certain RCM skill sensitivities to ICs, causing internal variability that may modulate or even mask physically forced signals (Giorgi and Bi [5]). LBC plays a critical role in RCM simulations, while IC impacts generally decreases with the simulation length (Wu *et al.* [7]). This study compares the relative contributions from uncertainties in ICs and LBCs to the RCM climate simulations for the 1998 summer China flood.

The study of ICs' effects on RCM through internal variability conducted by Giorgi and Bi [5] constructed different ICs and LBCs by adding random perturbations on the European Center for Medium-Range Weather Forecast (ECMWF) observational reanalysis (ERA; Gibson *et al.* [8]). In contrast, the present study uses 15 consecutive days during April 1-15 to initialize the RCM from the National Centers for Environmental Prediction Department of Energy (NCEP/DOE) Atmospheric Model Intercomparison Project (AMIP) II reanalysis (R-2; Kanamitsu *et al.* [9]) to depict the IC uncertainties. LBCs uncertainties are specified by differences among R-2, ERA, ERA Interim reanalysis (ERI, Dee *et al.* [10]) and Japanese 25-year reanalysis (JRA, Onogi *et al.* [11]). The RCM sensitivities to these ICs and LBCs uncertainties are investigated for the summer of 1998 when severe flooding occurred along the Yangtze River Basin. This case has been identified with active convection at regional to local scales under strong anomalous planetary forcings (Samel and Liang [12]) and thus is ideal for

\*Address correspondence to this author at the Earth System Science Interdisciplinary Center, University of Maryland, 5825 University Research Court Suite 4001, College Park, MD 20740, USA; Tel: 301 405-1522; Fax: 301 405-8468; E-mail: liusy@umd.edu

evaluation of RCM performance (Wang *et al.* [13]; Liu *et al.* [14, 15]).

Section 2 describes the model configuration and experiment design. Section 3 and 4 depict the RCM result dependence on ICs and LBCs focusing on precipitation and surface air temperature. Section 5 gives the conclusion.

## 2. MODEL CONFIGURATION AND EXPERIMENT DESIGN

The RCM for this study is the RegCM3 (Elguindi *et al.* [16], available from <http://users.ictp.it/~pubregcm/RegCM3/>), which is widely used for regional climate downscaling over China (Wang *et al.* [13]; Liu *et al.* [14, 15]). It was developed from the fifth-generation Pennsylvania State University-National Center for Atmospheric Prediction (PSU-NCAR) Mesoscale Model (MM5) hydrostatic dynamic core coupled with physics parameterization schemes suitable for climate applications (Dudhia *et al.* [17]).

The physics configuration chosen in this study is as follows. Cumulus convection is parameterized by the Grell [18] scheme. Non-convective precipitation and clouds are resolved by the explicit microphysics scheme of Pal *et al.* [19]. The longwave and shortwave radiative transfer is represented by the National Center for Atmospheric Research (NCAR) Community Climate Model (CCM3) scheme (Kiehl *et al.* [20]). The planetary boundary layer is treated by the nonlocal diffusion scheme of Holtslag and Boville [21]. The land surface processes are modeled by the Biosphere-Atmosphere Transfer Scheme version 1e (BATS; Dickinson *et al.* [22]). The U.S. Geological Survey (USGS) 10-min topographic data, and the BATS 20 vegetation

classifications are used to define, respectively, the representative terrain height and the dominant land cover for each grid box.

The RCM has 18 vertical layers with the model top at 100 hPa (~16.3 km above the sea level). Its computational domain is centered at (35.18 °N, 110 °E) and covers China by a 30-km horizontal grid distance using the Lambert conformal map projection. Fig. (1) illustrates the domain design. The buffer zones are located across 12 grids along each of the 4 domain edges, where LBCs are specified throughout the integration period using a dynamic relaxation technique (Giorgi *et al.* [23]). This domain has been shown to produce the most skillful simulation of the 1998 summer precipitation distribution over China (Liu *et al.* [14, 15]). Outlined in Fig. (1) are also four key regions (South, Yangtze River Basin, North, and Northeast) that have been identified as having distinct climate regimes and precipitation characteristics relating to the China summer monsoon precipitation (Mei-yu) (Ding [24]). Generally, the Mei-yu rainband arrives in the South during late May and early June, advances to the Yangtze River Basin in middle and late June, and then to the North in July, and to the Northeast in August (Samel *et al.* [25]). This study will elaborate model result sensitivities over these representative regions.

To depict the effect of IC uncertainties, 15 RCM runs were conducted for continuous integrations starting consecutively from April 1 to 15 while all ending on September 1, 1998. These ICs are provided by the same R-2 that constructs the LBCs during the entire integration period. Thus, a set of 15 realizations that differ only by their initial

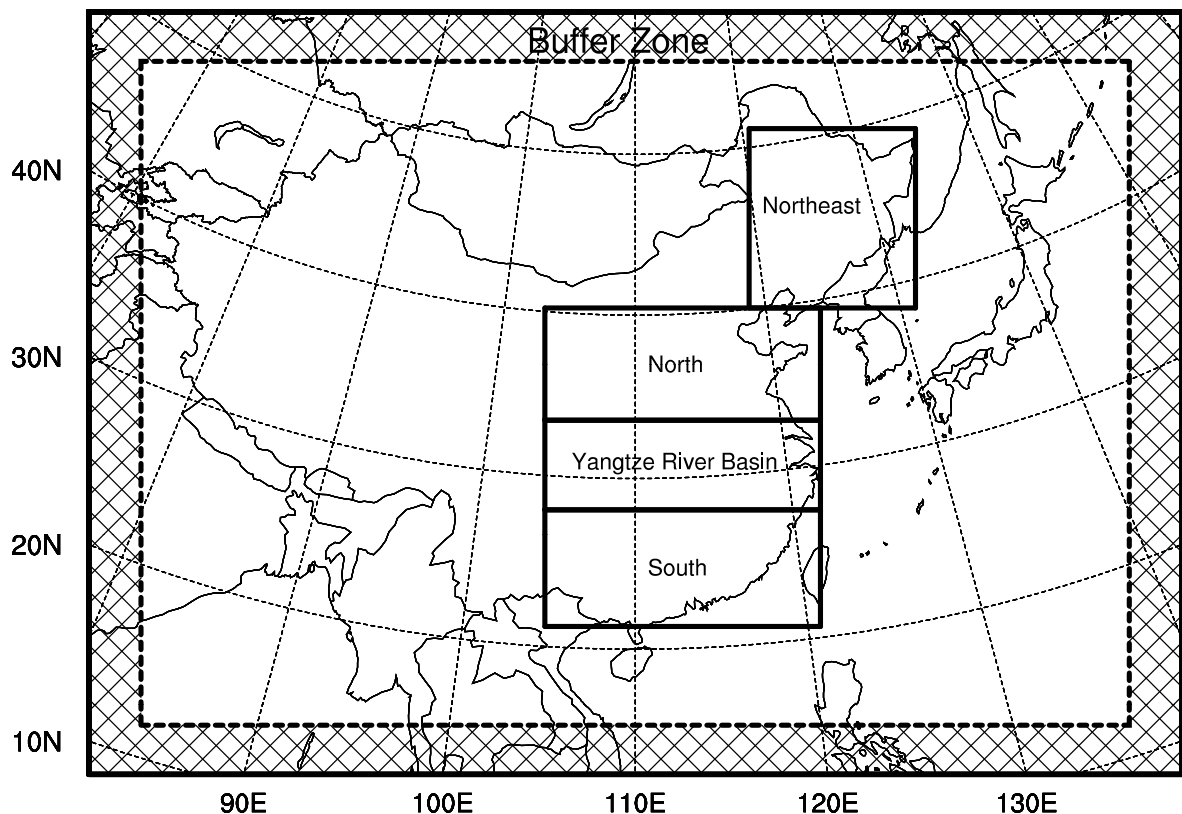
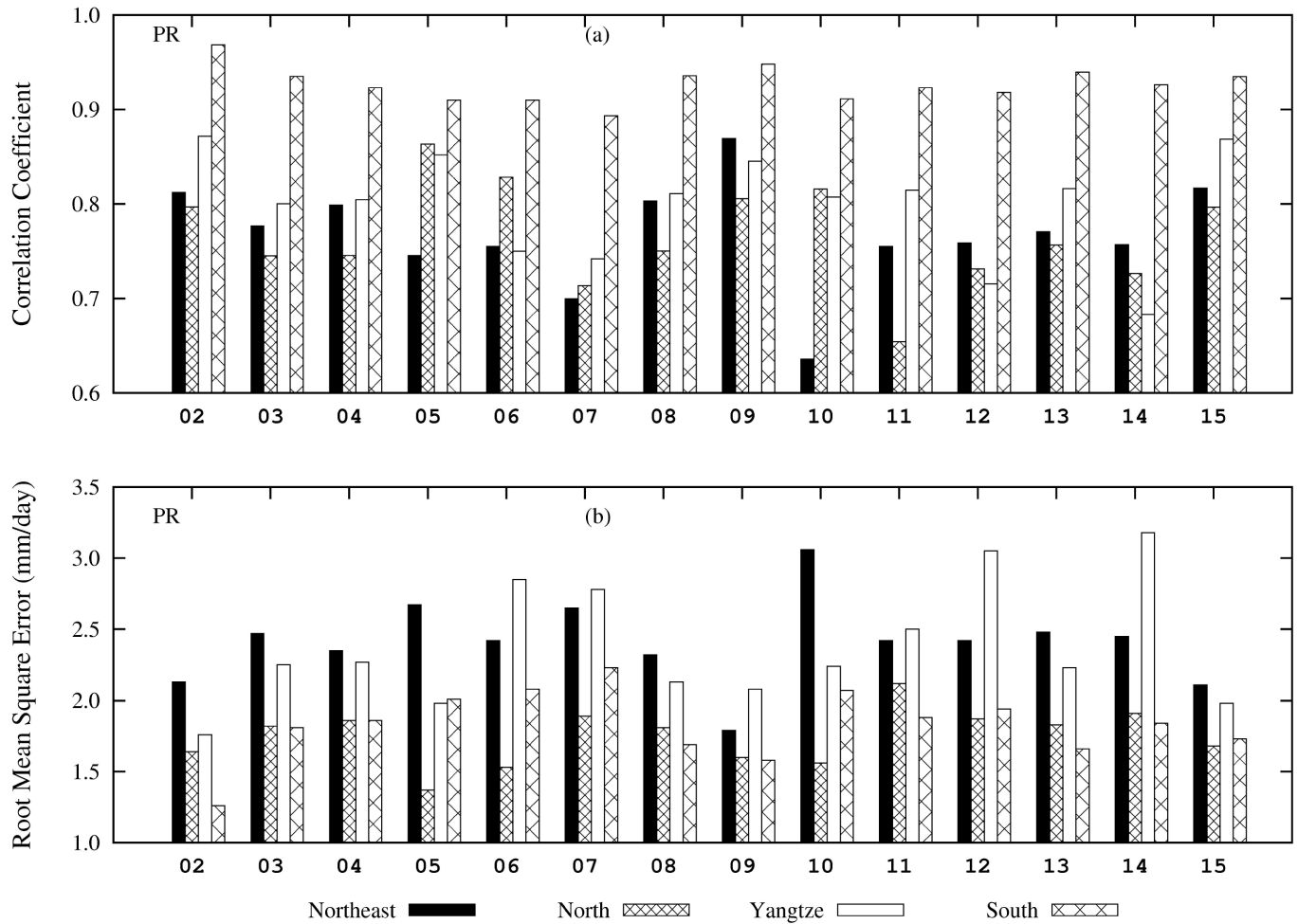


Fig. (1). Computational domain and 4 sub-regions (Northeast, North, Yangtze River Basin and South). Hatched lines denote the buffer zones where LBCs are specified.



**Fig. (2).** The correlation coefficient (a) and root mean square error (mm day<sup>-1</sup>, b) daily mean precipitation variations between observation and each of the 15 cases during June, July and August averaged over the Northeast, North, Yangtze River Basin and South.

conditions can be used to determine the RCM skill dependence on ICs. To study the effect of LBC uncertainties, additional experiments were conducted using R-2, ERA, ERI and JRA, all starting on April 1 and ending on September 1, 1998. The temporal interval is 6 hour for all the four reanalyses. The spatial grid varies while all using equal longitude × latitude, 2.5° for R-2 and ERA, 1.5° for ERI, and 1.25° for JRA. These simulations are compared to determine the RCM skill dependence on the uncertainties induced by LBCs. All the analyses are based on the RCM simulations of June, July and August.

**3. RCM SKILL DEPENDENCE ON ICs**

Precipitation and surface air temperature are the key variables generally used for RCM skill evaluation. The simulation started from April 1 is referred to as the control experiment (case 01), all other 14 realizations initialized from April 2 to 15 are compared with case 01 to depict the effect of ICs since they all are driven by identical LBCs. Fig. (2) illustrates the correlation coefficients (CC) and root mean square errors (RMS) for daily mean precipitation variations between case 01 and each of the 14 runs during June, July and August averaged over the Northeast, North, Yangtze River basin, and South (Fig. 1).

As compared with case 01, the South has the highest CC for all runs, between 0.89 (case 07) and 0.97 (case 02). In contrast, Northeast has the lowest CC, between 0.64 (case 10) and 0.87 (case 09), both of which are much lower than those for South. Consistently, South generally has the lowest RMS between 1.26 (case 02) – 2.23 (case 07) mm day<sup>-1</sup>, while the Northeast has highest RMS between 1.79 (case 09) – 3.06 (case 10) mm day<sup>-1</sup>. There exists no obvious relationship of either CC scores or RMS errors with starting dates for all the four regions.

The 1998 summer flood was induced by severe rainfall events which were mainly determined by convective processes in the South. On the other hand, precipitation in the Northeast is largely generated through synoptic weather processes, such as front passages and cyclone activities. As a result, the precipitation simulation in the South is less sensitive to ICs producing much higher CC than the Northeast.

Fig. (3) shows the same statistics for surface air temperature as that for precipitation. The Northeast has the highest CC for all 14 runs while the Yangtze River Basin has the lowest CC for most runs. The CC ranges among the 14 runs for the four regions, however, are generally very small, indicating that the sensitivity of surface air temperature simulation to ICs is weak. As for RMS, the South has the

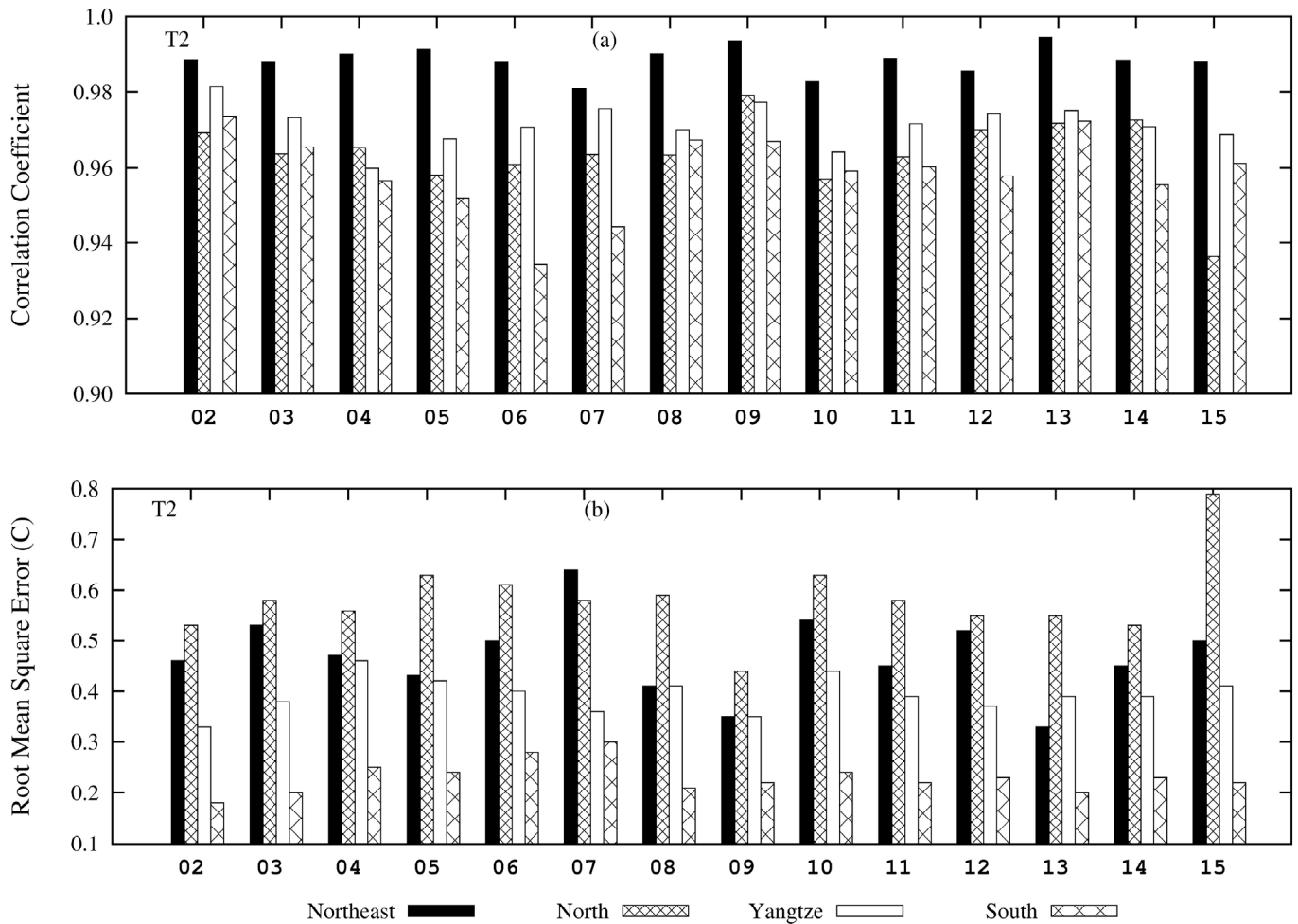


Fig. (3). The correlation coefficient (a) and root mean square error (°C, b) daily mean surface air temperature variations between observation and each of the 15 cases during June, July and August averaged over the Northeast, North, Yangtze River Basin and South.

smallest values for all 14 runs, while the North has the largest values for all the cases except 07. The RMS ranges are also very small among the 14 runs for the four regions. The smaller CC and RMS ranges showed in Fig. (3) than those in Fig. (2) suggest that ICs have much less effect on surface air temperature than precipitation, which are consistent with previous studies (Giorgi and Bi [5]; Christensen *et al.* [26]).

A question is whether the ensemble mean of all runs with perturbed ICs improves the RCM performance over the individual realizations. Fig. (4) compares with observations the geographical distributions of 1998 summer (June, July and August) mean precipitation and surface air temperature for case 01 (R-2, hereafter), and the ensemble average (IC\_ENS) of all 15 runs. The patterns for the R-2 and IC\_ENS closely resemble each other for both precipitation and surface air temperature. Both fail to reproduce the southwest-northeast main rainbelt along the Yangtze River Basin, but successfully simulate the South and Northeast centers. Both can depict the general temperature pattern (e.g., the warm center over the Yangtze River Basin and North China, Sichun Basin), but produce systematic cold biases of 4°C. A comparison of the spatial frequency distribution for summer mean biases in precipitation and

surface air temperature over all grids east of 100°E, where observations are abundant, shows no overall difference between IC\_ENS and R-2 and all other IC runs. These results indicate that the ensemble mean has little improvement than individual realizations as far as the 1998 summer seasonal averages concerned.

Fig. (5) compares daily mean precipitation variations during June 1 – August 30 averaged over the four regions between the R-2 and IC\_ENS with observations. Again, the R-2 and ENS closely resemble each other over all regions. The correlations with observations over the Northeast, North, Yangtze River Basin, South are 0.01, 0.34, 0.37, 0.39 for the R-2 and 0.02, 0.37, 0.45, 0.39 for the IC\_ENS. Thus the IC effect is small even for daily precipitation evolution. This is more so for surface air temperature.

All of the above statistical measures demonstrate that the effect of perturbed ICs is trivial, and thus their ensemble mean shows little improvement in the RCM downscaling skill. This results from the dominant control by the driving LBCs throughout the entire integration period. The effect from IC perturbations quickly dissipates and plays minor role after the spin-up period, typically of ~10 days (Giorgi and Means [27]; Wu *et al.* [7]).

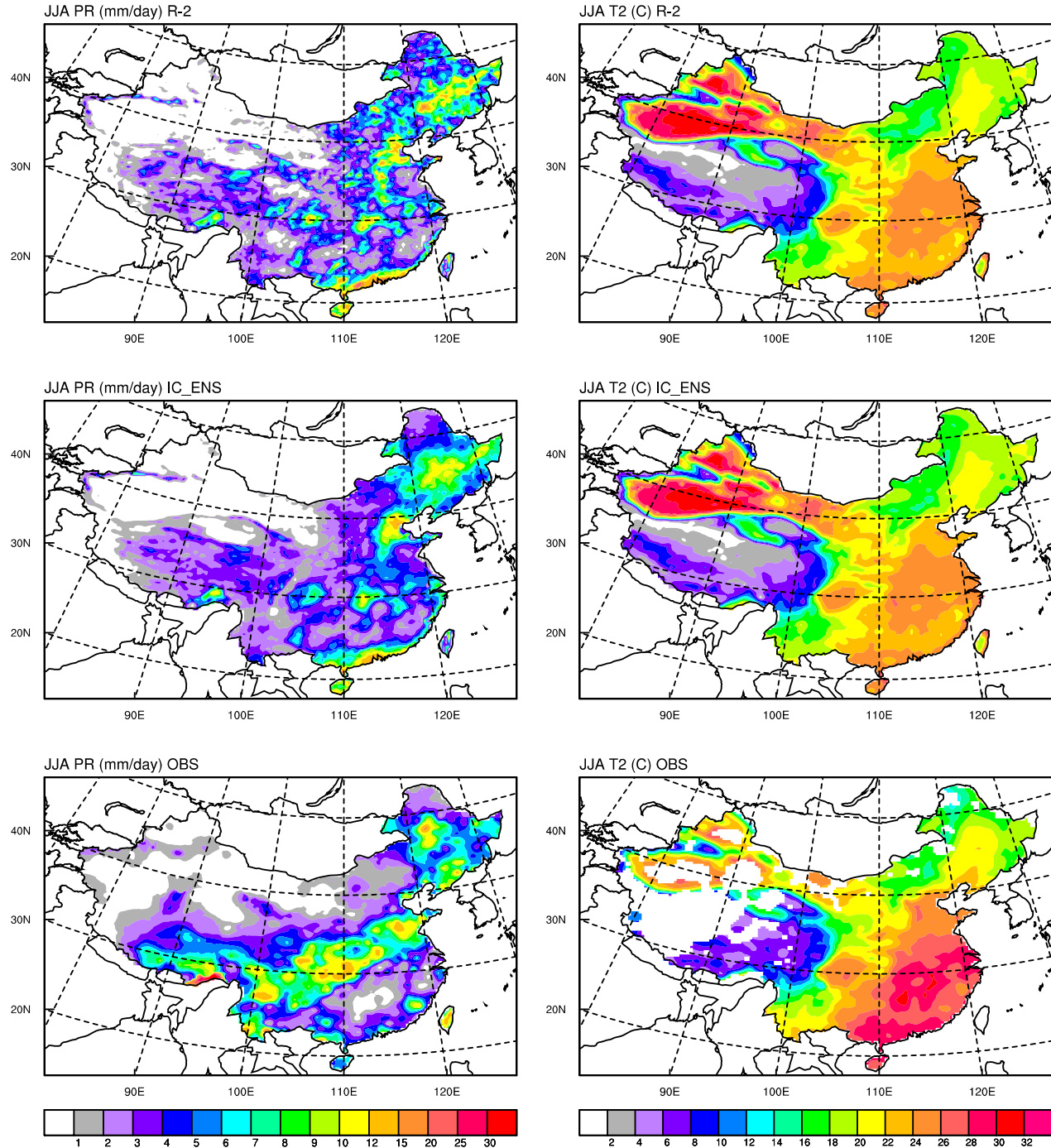


**Fig. (4).** Geographical distributions of summer mean precipitation ( $\text{mm day}^{-1}$ , *left*) and surface air temperature ( $^{\circ}\text{C}$ , *right*). Simulated in case 01 (R-2, *top*), as the ensemble mean of 15 runs (IC\_ENS, *middle*) and observed (OBS, *bottom*).

**4. RCM SKILL DEPENDENCE ON LBCs**

The RCM downscaling results are constrained by the large-scale atmospheric circulation forcings through dynamic relaxation of the LBCs. The RCM domain has been objectively chosen to correctly represent the internal mesoscale physical processes while minimizing the impact of LBC errors such that the observed spatial distributions

and temporal variations of near surface climate can be realistically simulated at regional-local scales (Liang *et al.* [4]; Liu *et al.* [14]). The LBC errors which are from large-scale reanalyses uncertainties, however, can still be transferred into the RCM domain to affect the downscaling skill. Fig. (6) shows 925 hPa relative humidity correlation coefficients between R-2 and ERA, ERI, JRA based on daily averages during June 1 – August 30, the values for

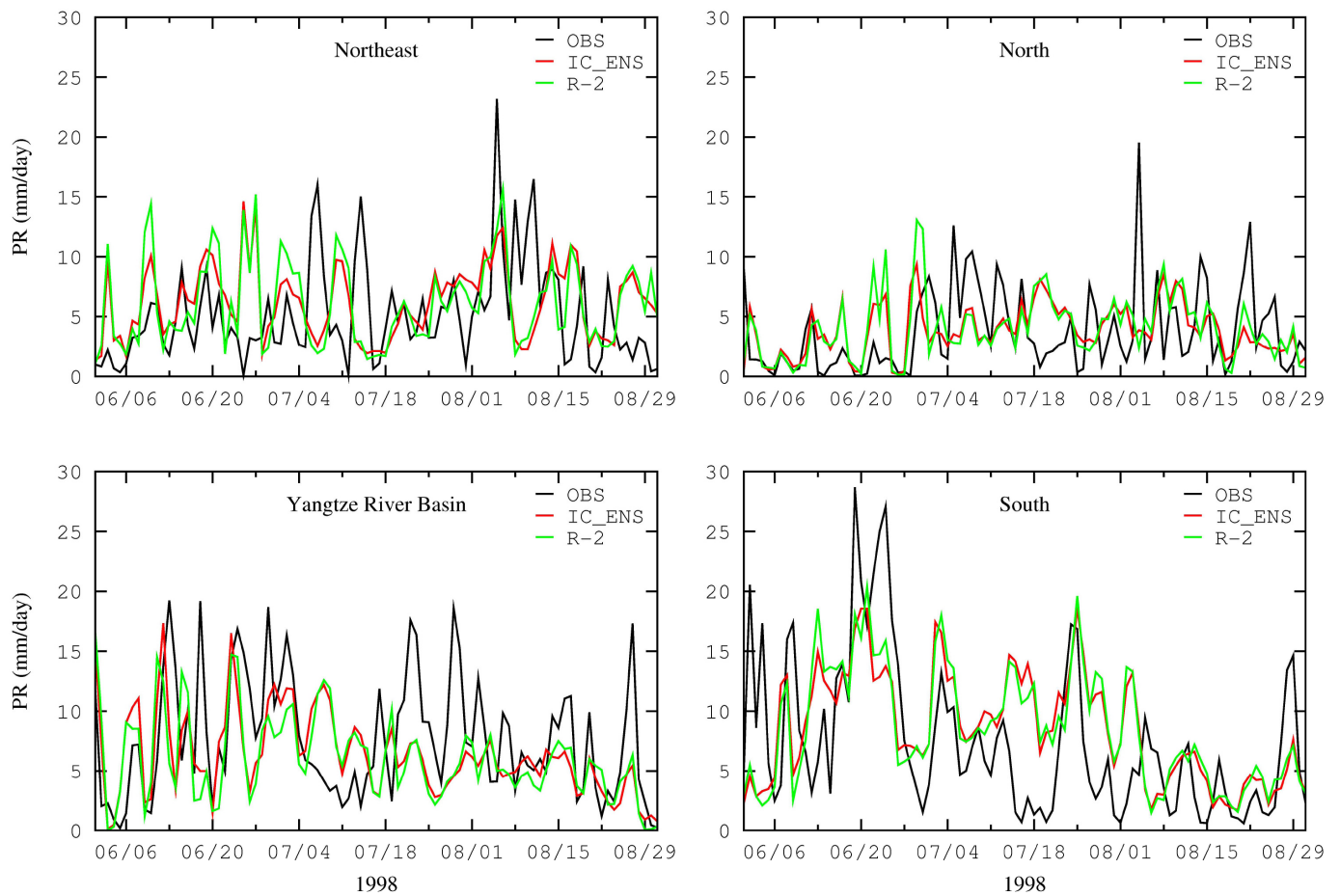


**Fig. (5).** Daily mean precipitation variations during June 1 to August 30 averaged over the four key regions for observations (OBS), ensemble mean (IC\_ENS) and case 01 (R-2).

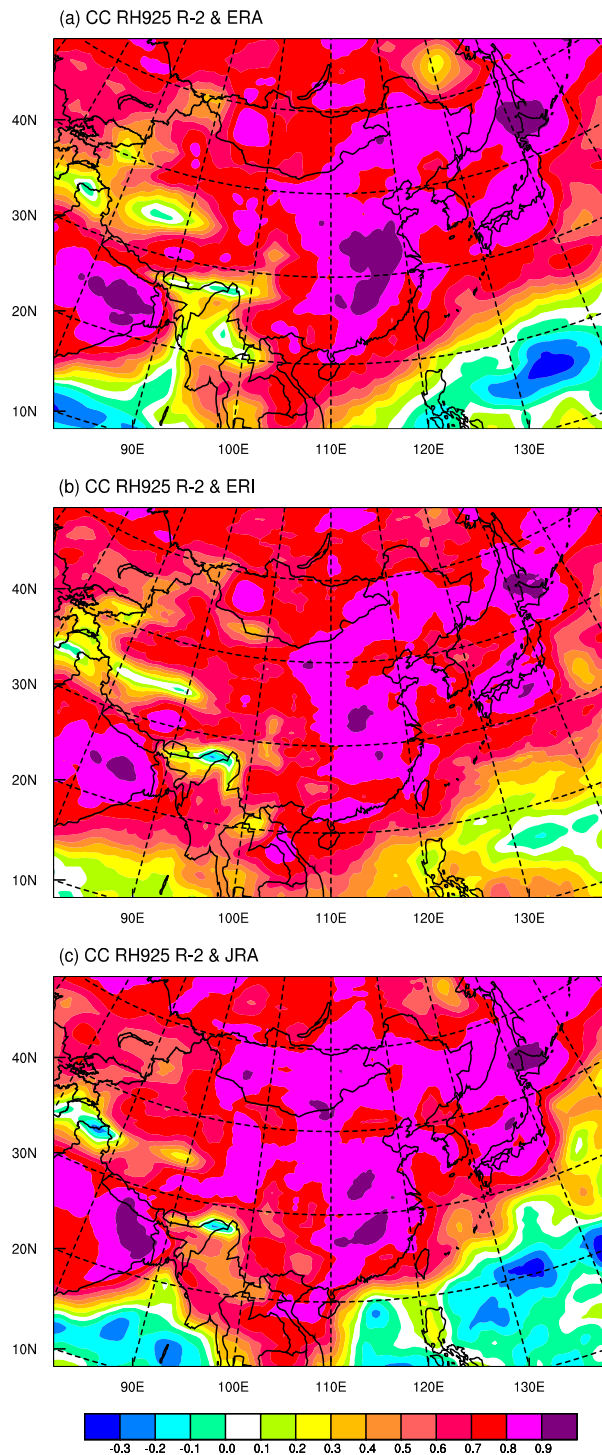
confidence level 95% and 99% by Student's one-sided t-test are 0.21 and 0.27 respectively. The three correlation coefficient fields showed similar geographical distribution patterns. Correlation coefficient that passed the 99% confidence level mainly occurred over land except Tibet Plateau. Most of the east China where observations are abundant has high values that are over 0.8 or even 0.9. Very low even negative correlation coefficient values are occurred over tropical oceans and failed to pass the 95% confidence level. These substantial differences indicate inconsistency between the large-scale reanalyses, typically over the areas where observational data are lacking. LBCs constructed from these large-scale reanalyses within the problematic areas resulted in LBC errors which are integrated into the RCM domain and impact the RCM performance.

Fig. (7) compares daily mean precipitation variations during June 1 – August 30 averaged over the four regions as observed and downscaled by the RCM from the R-2, ERA, ERI, JRA as well as the ensemble averages (LBC\_ENS) of the four runs. Over the Northeast, large discrepancies between the RCM simulations mainly occurred during the end of June and early July, where all runs and the ensemble average failed to reproduce the observation. On the other hand, over the North, the differences between individual runs and LBC\_ENS are small in June and July, but larger in August. Over the Yangtze River Basin, the discrepancies

between the runs are large in June, while relatively small in July and August. Over the South, large spreads between the runs occurred throughout the whole summer.

Table 1 lists the CC and RMS scores of the regional mean daily precipitation and surface air temperature downscaled by the RCM from 4 reanalyses as compared with observations. For precipitation, all runs has poor performance over the Northeast and North (failed to pass the Student's one-sided t-test 95% confidence level), while over the Yangtze River Basin and South, the simulation driven by the R-2 is the best (passed the 99% confidence level). Especially over the South, the R-2 driven run has CC of 0.45, much higher than other runs and the ensemble average. For surface air temperature, both the CC and RMS measures indicate substantially better skill scores (all passed 99% confidence level) and smaller spreads among runs than precipitation. For both precipitation and temperature, the ensemble mean does not improve the RCM skill over the individual runs driven by R-2, ERA, ERI or JRA.

The effect of LBC uncertainties on precipitation is the largest over the Northeast and smallest over the South, which is similar to that of IC uncertainties. This regional contrast occurs because precipitation is mainly produced by local convective processes in the South rather than by synoptic weather systems in the Northeast as controlled by large-scale circulations.



**Fig. (6).** Geographical distribution of correlation coefficient (CC) for relative humidity (RH) on 925 hPa between R-2 and ERA (a), ERI (b) and JRA (c).

Fig. (8) shows the geographical distributions of summer mean precipitation downscaled by the RCM from ERA, ERI, JRA reanalyses and the ensemble average of the four RCM runs (LBC\_ENS). They can be compared with the R-2 and observations in Fig. (4). In contrast to the IC perturbations that generate little sensitivity, the LBCs from the R-2, ERA,

ERI and JRA produce notable differences in precipitation geographic distributions. In particular, the R-2 run has less precipitation than all other runs over the Northeast, North and South. All runs driven and their ensemble average fail to reproduce the observed main rainbelt oriented from the southwest to northeast over the Yangtze River Basin. The R-2 LBCs drive the RCM to result in more realistic downscaling over the South where the other three forcings (especially ERA) lead to excessive precipitation. Again, the ensemble average of the four runs does not improve the overall RCM downscaling performance.

## 5. DISCUSSION AND CONCLUSION

The RegCM3 downscaling skill dependence on initial conditions is examined by comparing summer simulations driven by R-2 starting from consecutive dates from April 1 – 15, 1998. The results showed that the IC perturbations have certain influences on daily variations of precipitation and surface air temperature, but little effect on seasonal mean geographical distributions. The ensemble mean of the 15 runs does not produce overall superior RCM skill to individual realizations. Simulation of precipitation is more sensitive to ICs than surface air temperature.

On the other hand, the RegCM3 exhibits stronger dependence on LBC forcings than IC perturbations. Four simulations driven by R-2, ERA, ERI and JRA, all starting on April 1, contain large discrepancies in both daily variations and summer mean geographical distributions of precipitation. The RegCM3 driven by the ERA generally produces more precipitation than that by the R-2, ERI and JRA over most of the domain. The ensemble mean of the four runs has little skill enhancement to the individuals.

The above conclusion has two important limitations. First, our results on both IC and LBC ensemble means were based on simple averaging (with an equal weight) of all realizations. They did not produce significant skill enhancement to individual realizations. On the other hand, the optimized physics ensemble is likely an effective approach to achieve significant skill improvement, especially for precipitation as demonstrated by Liang *et al.* [28] and Liu *et al.* [15]. Second, the RCM downscaling skill also strongly depends on model physics, especially the parameterizations of subgrid processes like cumulus convection (Liang *et al.* [28]). For short-range synoptic-scale precipitation forecasts, Clark *et al.* [29] found that model errors due to physics representations are greater than those from IC or LBC uncertainties. The sensitivity of RCM physics configuration and the optimization of ensemble weighting require further investigation. While improve RCM skill through initial and lateral boundary conditions and their ensemble are not recommended.

## ACKNOWLEDGEMENTS

This research was supported in part by the USDA Cooperative State Research, Education, and Extension Service (CSREES) AG CSU G-1469-1 and the NOAA Education Partnership Program (EPP) COM Howard 631017. The views expressed are those of the authors and do not necessarily reflect those of the sponsoring agencies and the Earth System Science Interdisciplinary Center.

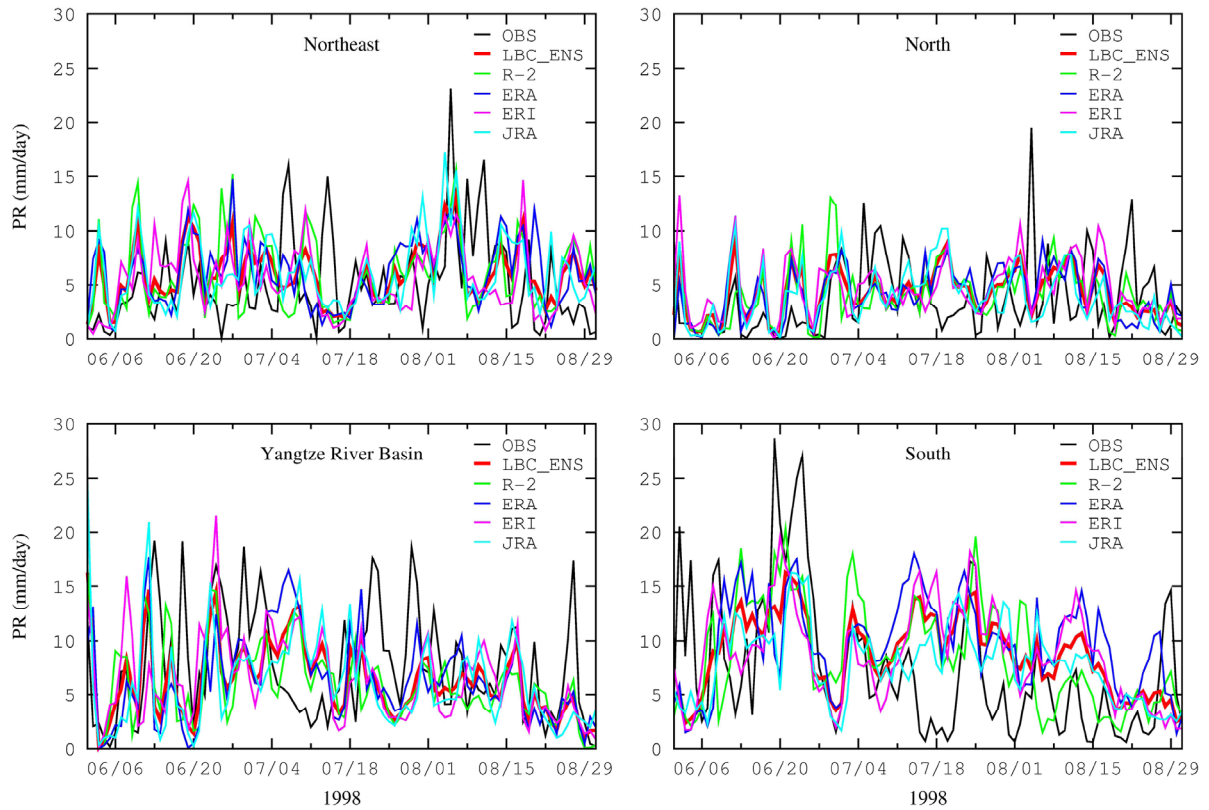
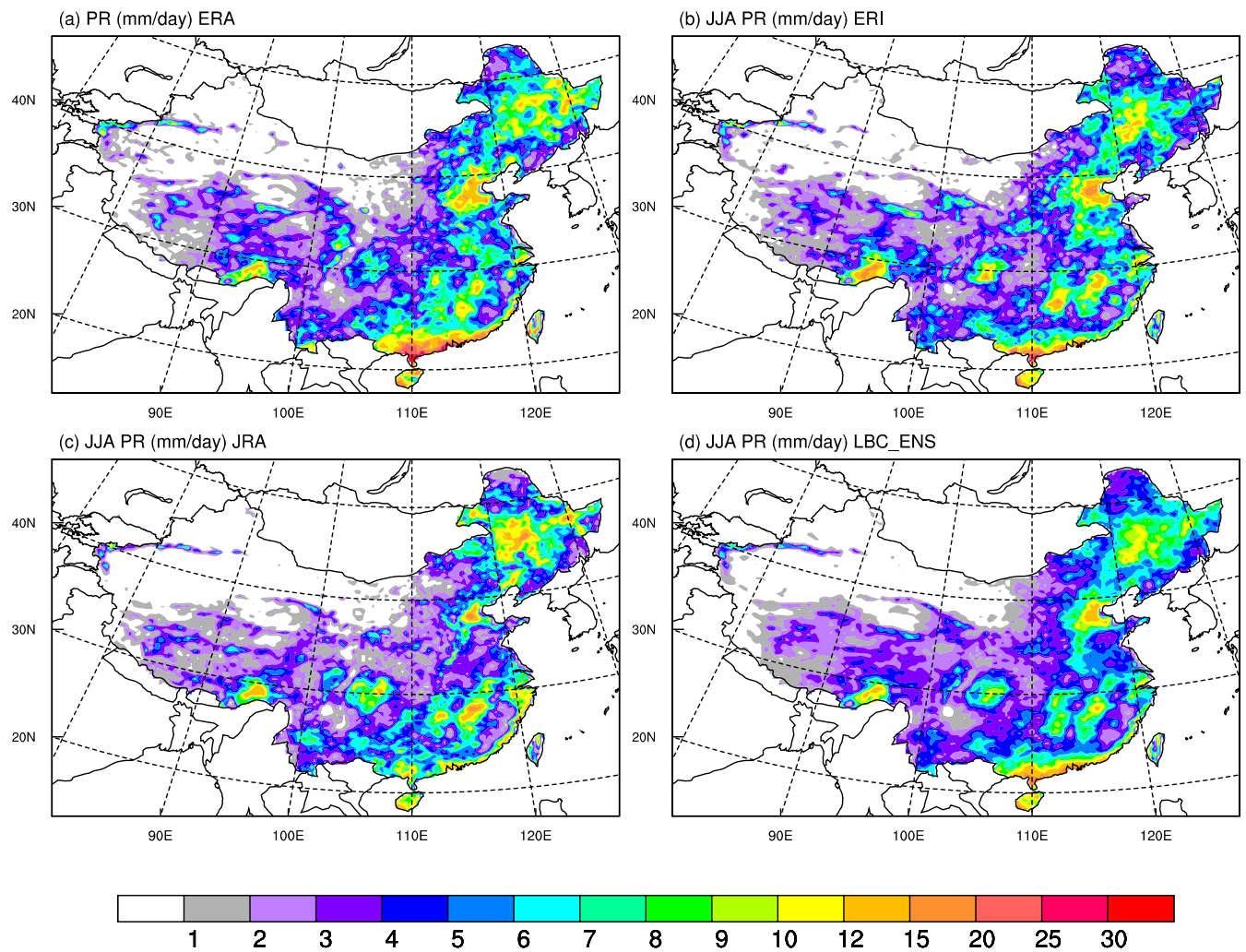


Fig. (7). Daily mean precipitation variations during June 1 to August 30 averaged over the four key regions for observations (OBS), RCM simulates driven by the R-2, ERA, ERI and JRA as well as their ensemble mean (LBC\_ENS).

Table 1. Statistics of Precipitation and Surface Air Temperature Downscaled by the RCM from the R-2, ERA, ERI and JRA as well as the Ensemble Mean of the Four Runs (LBC\_ENS). Shown are Correlation Coefficients (CC) and Root Mean Square Error (RMS) of Simulated with Observed Daily Means Averaged Over the Four Key Regions

		Precipitation		Surface Air Temperature	
		CC	RMS (mm day <sup>-1</sup> )	CC	RMS (°C)
Northeast	R-2	<i>0.01*</i>	5.56	0.80	2.62
	ERA	<i>0.15</i>	4.90	0.82	2.53
	ERI	<i>0.15</i>	4.87	0.84	2.16
	JRA	<i>0.14</i>	4.98	0.82	2.30
	LBC_ENS	<i>0.13</i>	4.68	0.83	2.37
North	R-2	<i>0.12</i>	4.19	0.70	2.21
	ERA	<i>0.09</i>	4.18	0.71	2.21
	ERI	<i>0.03</i>	4.44	0.72	2.30
	JRA	<i>0.13</i>	4.14	0.68	2.17
	LBC_ENS	<i>0.11</i>	3.98	0.73	2.14
Yangtze River Basin	R-2	0.28	5.44	0.68	2.85
	ERA	0.18	5.94	0.66	2.70
	ERI	<b>0.26**</b>	5.55	0.56	2.87
	JRA	0.14	6.29	0.68	2.73
	LBC_ENS	<b>0.25</b>	5.39	0.67	2.75
South	R-2	0.45	6.13	0.67	3.33
	ERA	0.15	7.48	0.62	3.03
	ERI	0.30	6.72	0.66	3.14
	JRA	0.34	6.20	0.70	3.04
	LBC_ENS	0.38	6.17	0.70	3.12

\*Italic numbers indicate the correlation coefficient failed to pass the Student's one-sided t-test 95% confidence level.  
 \*\* Bold numbers indicate the correlation coefficient failed to pass the Student's one-sided t-test 99% confidence level.



**Fig. (8).** Geographical distribution of summer mean precipitation ( $\text{mm day}^{-1}$ ) simulated driven by ERA (a), ERI (b), JRA (c) and as the ensemble average (LBC\_ENS, (d)) of the four runs driven by R-2, ERA, ERI and JRA.

## CONFLICT OF INTEREST

None declare.

## REFERENCES

- [1] Lorenz EN. A study of the predictability of a 28-variable atmospheric model. *Tellus* 1965; 17: 321-33.
- [2] Toth Z, Kalnay E. Ensemble forecasting at NMC: the generation of perturbations. *Bull Am Meteorol Soc* 1993; 74: 2317-30.
- [3] Mullen SL, Du J, Sanders F. The dependence of ensemble dispersion on analysis forecast system implications to short-range ensemble forecasting of precipitation. *Mon Weather Res* 1999; 127: 1674-86.
- [4] Liang X-Z, Kunkel KE, Samel AN. Development of a regional climate model for U.S. Midwest applications. Part I: sensitivity to buffer zone treatment. *J Climate* 2001; 14: 4363-78.
- [5] Giorgi F, Bi X. A study of internal variability of a regional climate model. *J Geophys Res* 2000; 105: 29503-21.
- [6] Warner TT, Peterson RA, Treadon RE. A tutorial on lateral boundary conditions as a basic and potentially serious limitation to regional numerical weather prediction. *Bull Am Meteorol Soc* 1997; 78: 2599-617.
- [7] Wu W, Lynch AH, Rivers A. Estimating the uncertainty in a regional climate model related to initial and lateral boundary conditions. *J Climate* 2005; 18: 917-33.
- [8] Gibson JK, Källberg P, Uppala S, *et al.* ERA description. ECMWF Re-Analysis Project Report Series, No. 1, ECMWF, Reading, United Kingdom 1997.
- [9] Kanamitsu M, Ebisuzaki W, Woolen J, *et al.* The NCEP-DOE AMIP-II reanalysis (R-2). *Bull Am Meteorol Soc* 2002; 83: 1631-43.
- [10] Dee DP, Uppala SM, Simmons AJ, *et al.* The ERA-Interim reanalysis: configuration and performance of the data assimilation system. *Q J R Meteorol Soc* 2011; 137: 553-97.
- [11] Onogi K, Tsutsui J, Koide H, *et al.* The JRA-25 Reanalysis. *J Meteorol Soc Japan* 2007; 85: 369-432.
- [12] Samel AN, Liang X-Z. Understanding relationships between the 1998 Yangtze River flood and northeast Eurasian blocking. *Climate Res* 2003; 23: 149-58.
- [13] Wang YQ, Sen OL, Wang B. A highly resolved regional climate model (IPRC-RegCM) and its simulation of the 1998 severe precipitation event over China. Part I: Model description and verification of simulation. *J Climate* 2003; 16: 1721-38.
- [14] Liu S, Liang X-Z, Gao W, Zhang H. Application of climate-weather research and forecasting model (CWRf) in China: domain optimization. *Chin Atmos Sci* 2008; 32: 457-68.
- [15] Liu S, Gao W, Xu M, Wang X, Liang X-Z. China summer precipitation simulations using an optimal ensemble of cumulus schemes. *Front Earth Sci China* 2009; 3: 248-57.
- [16] Elguindi N, Bi X, Giorgi F, *et al.* RegCM Version 3.1 User's Guide, 2007. Available from: <http://users.ictp.it/~pubregcm/RegCM3/>

- [17] Dudhia J, Gill D, Guo YR, Manning K, Wang W, Chriszar J. PSU/NCAR mesoscale modeling system tutorial class notes and user's guide: MM5 modeling system Version 3, 2000. Available from: <http://www.mmm.ucar.edu/mm5/doc.html>
- [18] Grell G. Prognostic evaluation of assumptions used by cumulus parameterizations. *Mon Weather Rev* 1993; 121: 764-87.
- [19] Pal JS, Small EE, Eltahir EAB. Simulation of regional-scale water and energy budgets: representation of subgrid cloud and precipitation processes with RegCM. *J Geophys Res* 2000; 105(D24): 29579-94.
- [20] Kiehl JT, Hack JJ, Bonan GB, *et al.* Description of the NCAR community climate model (CCM3). NCAR Tech. Note NCAR/TN-420+STR, National Center for Atmospheric Research, Boulder, Colorado, 1996; pp. 152.
- [21] Holtslag AAM, Boville BA. Local versus nonlocal boundary-layer diffusion in a global climate model. *J Climate* 1993; 6: 1825-42.
- [22] Dickinson RE, Henderson-Seller A, Kennedy PJ. Biosphere-Atmosphere Transfer Scheme (BATS) version 1e as coupled to the NCAR community climate model. NCAR Tech Note NCAR/TN-387+STR, National Center for Atmospheric Research, Boulder, CO, 1993; 72.
- [23] Giorgi F, Marinucci MR, Bates GT. Development of a second generation regional climate model (RegCM2) II: Convective processes and assimilation of lateral boundary conditions. *Mon Weather Rev* 1993; 121: 2814-32.
- [24] Ding YH. Summer monsoon rainfall in China. *J Meteorol Soc Jpn* 1991; 70: 243-66.
- [25] Samel AN, Wang WC, Liang X-Z. The monsoon rainband over China and relationship with the Eurasian circulation. *J Climate* 1999; 12:115-31.
- [26] Christensen OB, Gaertner MA, Prego JA, Polcher J. Internal variability of a regional climate model. *Clim Dyn* 2001; 17: 875-87.
- [27] Giorgi F, Mearns LO. Introduction to special section: regional climate modeling revisited. *J Geophys Res* 1999; 104: 6335-52.
- [28] Liang X-Z, Xu M, Kunkel K-E. Regional climate model simulation of U.S.-Mexico summer precipitation using the optimal ensemble of two cumulus parameterizations. *J Climate* 2007; 20: 5201-7.
- [29] Clark AJ, Gallus WA Jr, Chen T-C. Contributions of mixed physics versus perturbed initial/lateral boundary conditions to ensemble-based precipitation forecast skill. *Mon Weather Rev* 2008; 136: 2140-56.

---

Received: July 26, 2011

Revised: September 7, 2011

Accepted: September 9, 2011

© Liu *et al.*; Licensee Bentham Open.

This is an open access article licensed under the terms of the Creative Commons Attribution Non-Commercial License (<http://creativecommons.org/licenses/by-nc/3.0/>) which permits unrestricted, non-commercial use, distribution and reproduction in any medium, provided the work is properly cited.